The Plant Cell, Vol. 26: 296–309, January 2014, www.plantcell.org

The *Arabidopsis* SIAMESE-RELATED Cyclin-Dependent Kinase Inhibitors SMR5 and SMR7 Regulate the DNA Damage Checkpoint in Response to Reactive Oxygen Species[W]

Dalong Yi,[a,b,1] Claire Lessa Alvim Kamei,[a,b,1,2] Toon Cools,[a,b] Sandy Vanderauwera,[a,b] Naoki Takahashi,[c] Yoko Okushima,[c] Thomas Eekhout,[a,b] Kaoru Okamoto Yoshiyama,[c] John Larkin,[d] Hilde Van den Daele,[a,b] Phillip Conklin,[e] Anne Britt,[e] Masaaki Umeda,[c,f] and Lieven De Veylder[a,b,3]

[a] Department of Plant Systems Biology, VIB, B-9052 Gent, Belgium
[b] Department of Plant Biotechnology and Bioinformatics, Ghent University, B-9052 Gent, Belgium
[c] Graduate School of Biological Sciences, Nara Institute of Science and Technology, Nara 630-0192, Japan
[d] Department of Biological Sciences, Louisiana State University, Baton Rouge, Louisiana 70803
[e] Department of Plant Biology, University of California Davis, Davis, California 95616
[f] JST, Core Research for Evolutional Science and Technology, Nara 630-0192, Japan

Whereas our knowledge about the diverse pathways aiding DNA repair upon genome damage is steadily increasing, little is known about the molecular players that adjust the plant cell cycle in response to DNA stress. By a meta-analysis of DNA stress microarray data sets, three family members of the *SIAMESE/SIAMESE-RELATED* (*SIM/SMR*) class of cyclin-dependent kinase inhibitors were discovered that react strongly to genotoxicity. Transcriptional reporter constructs corroborated specific and strong activation of the three *SIM/SMR* genes in the meristems upon DNA stress, whereas overexpression analysis confirmed their cell cycle inhibitory potential. In agreement with being checkpoint regulators, *SMR5* and *SMR7* knockout plants displayed an impaired checkpoint in leaf cells upon treatment with the replication inhibitory drug hydroxyurea (HU). Surprisingly, HU-induced *SMR5/SMR7* expression depends on ATAXIA TELANGIECTASIA MUTATED (ATM) and SUPPRESSOR OF GAMMA RESPONSE1, rather than on the anticipated replication stress-activated ATM AND RAD3-RELATED kinase. This apparent discrepancy was explained by demonstrating that, in addition to its effect on replication, HU triggers the formation of reactive oxygen species (ROS). ROS-dependent transcriptional activation of the *SMR* genes was confirmed by different ROS-inducing conditions, including high-light treatment. We conclude that the identified *SMR* genes are part of a signaling cascade that induces a cell cycle checkpoint in response to ROS-induced DNA damage.

INTRODUCTION

Being sessile, plants are continuously exposed to changing environmental conditions that can impose biotic and abiotic stresses. One of the consequences observed in plants subjected to altered growth conditions is the disruption of reactive oxygen species (ROS) homeostasis (Mittler et al., 2004). Under steady state conditions, ROS are efficiently scavenged by different non-enzymatic and enzymatic antioxidant systems, involving the activity of catalases, peroxidases, and glutathione reductases. However, when stress prevails, the ROS production rate can exceed the scavenging mechanisms, resulting in a cell- or tissue-specific rise in ROS. These oxygen derivatives possess a strong oxidizing potential that can damage a wide diversity of biological molecules, including the electron-rich bases of DNA, which results into single- and double-stranded breaks (DSBs; Amor et al., 1998; Dizdaroglu et al., 2002; Roldán-Arjona and Ariza, 2009). H_2O_2 is a major ROS compound and is able to transverse cellular membranes, migrating into different compartments. This feature grants H_2O_2 not only the potential to damage a variety of cellular structures, but also to serve as a signaling molecule, allowing the activation of pathways that modulate developmental, metabolic, and defense pathways (Mittler et al., 2011). One of the signaling effects of H_2O_2 is the activation of cell division arrest by cell cycle checkpoint activation (Tsukagoshi, 2012); however, the molecular mechanisms involved remain unknown.

Cell cycle checkpoints adjust cellular proliferation to changing growth conditions, arresting it by inhibiting the main cell cycle controllers: the heterodimeric complexes between the cyclin-dependent kinases (CDKs) and the regulatory cyclins (Lee and Nurse, 1987; Norbury and Nurse, 1992). The activators of these checkpoints are the highly conserved ATAXIA TELANGIECTASIA MUTATED (ATM) and ATM AND RAD3-RELATED (ATR) kinases that are recruited in accordance with the type of DNA damage (Zhou and Elledge, 2000; Abraham, 2001; Bartek and Lukas, 2001; Kurz and Lees-Miller, 2004). ATM is activated by DSBs, whereas ATR is activated by single-strand breaks or stalled replication forks,

[1] These authors contributed equally to this work.
[2] Current address: Wageningen UR-Plant Breeding, Wageningen University and Research Center, P.O. Box 386, 6700 AJ Wageningen, The Netherlands.
[3] Address correspondence to lieven.deveylder@psb.vib-ugent.be.
The author responsible for distribution of materials integral to the findings presented in this article in accordance with the policy described in the Instructions for Authors (www.plantcell.org) is: Lieven De Veylder (lieven.deveylder@psb.vib-ugent.be).
[W] Online version contains Web-only data.
www.plantcell.org/cgi/doi/10.1105/tpc.113.118943

causing inhibition of DNA replication. In mammals, ATM and ATR activation results in the phosphorylation of the Chk2 and Chk1 kinases, respectively. Both kinases subsequently phosphorylate p53, a central transcription factor in the DNA damage response (Chaturvedi et al., 1999; Shieh et al., 2000; Chen and Sanchez, 2004; Rozan and El-Deiry, 2007). Chk1, Chk2, and p53 seemingly appear to have no plant ortholog, although an analogous role for p53 is suggested for the plant-specific SUPPRESSOR OF GAMMA RESPONSE1 (SOG1) transcription factor that is under direct posttranscriptional control of ATM (Yoshiyama et al., 2009, 2013). Another distinct plant feature relates to the inactivation of CDKs in response to DNA stress. CDK activity is in part regulated by its phosphorylation status at the N terminus, determined by the interplay of the CDC25 phosphatase and the antagonistic WEE1 kinase, acting as the "on" and "off" switches of CDK activity, respectively (Francis, 2011). Whereas in mammals and budding yeast the activation of the DNA replication checkpoint, leading to a cell cycle arrest, is predominantly achieved by the inactivation of the CDC25 phosphatase, plant cells respond to replication stress by transcriptional induction of *WEE1* (De Schutter et al., 2007). In the absence of WEE1, *Arabidopsis thaliana* plants become hypersensitive to replication inhibitory drugs, such as hydroxyurea (HU), which causes a depletion of deoxynucleotide triphosphates (dNTPs) by inhibiting the ribonucleotide reductase (RNR) protein. However, *WEE1*-deficient plants respond similarly as control plants to other types of DNA damage (De Schutter et al., 2007; Dissmeyer et al., 2009). These data suggest the existence of yet to be identified pathways controlling cell cycle progression under DNA stress, operating independently of WEE1.

Potential candidates to operate in checkpoint activation upon DNA stress are CDK inhibitors (CKIs). CKI proteins are mostly low molecular weight proteins that inhibit cell division by their direct interaction with the CDK and/or cyclin subunit (Sherr and Roberts, 1995; De Clercq and Inzé, 2006). The first identified class of plant CKIs was the ICK/KRP (interactors of CDK/Kip-related protein) protein family comprising seven members in *Arabidopsis*, all sharing a conserved C-terminal domain being similar to the CDK binding domain of the animal CIP/KIP proteins (Wang et al., 1998, 2000; De Veylder et al., 2001). TIC (tissue-specific inhibitors of CDK) is the most recently suggested class of CKIs (DePaoli et al., 2012) and encompasses SCI1 (for STIGMA/STYLE CELL CYCLE INHIBITOR1) in tobacco (*Nicotiana tabacum*; DePaoli et al., 2011). SCI1 shares no apparent sequence similarity with the other classes of CKIs in plants and has been suggested to connect cell cycle progression and auxin signaling in pistils (DePaoli et al., 2012). The third class of CKIs is the plant-specific *SIAMESE/SIAMESE-RELATED* (*SIM/SMR*) gene family. SIM has been identified as a cell cycle inhibitor with a role in trichome development and endocycle control (Churchman et al., 2006). Based on sequence analysis, five additional gene family members have been identified in *Arabidopsis* and, together with EL2 from rice (*Oryza sativa*), have been suggested to act as cell cycle inhibitors modulated by biotic and abiotic stresses (Peres et al., 2007). Plants subjected to treatments inducing DSBs showed a rapid and strong induction of specific family members (Culligan et al., 2006; Adachi et al., 2011), suggesting that SIM/SMR proteins might include interesting candidates to complement WEE1 in the global response to DNA stress.

In this work, we identified three *SMR* genes (*SMR4*, *SMR5*, and *SMR7*) that are transcriptionally activated by DNA damage. Cell cycle inhibitory activity was demonstrated by overexpression analysis, whereas knockout data illustrated that both *SMR5* and *SMR7* are essential for DNA cell cycle checkpoint activation in leaves of plants grown in the presence of HU. Remarkably, we found that *SMR* induction mainly depends on ATM and SOG1, rather than ATR, as would be expected for a drug that triggers replication fork defects. Correspondingly, we demonstrate that the HU-dependent activation of *SMR* genes is triggered by ROS rather than replication problems, linking *SMR* genes with cell cycle checkpoint activation upon the occurrence of DNA damage-inducing oxidative stress.

RESULTS

Meta-Analysis of DNA Stress Datasets Identifies DNA Damage-Induced *SMR* Genes

When DNA damage occurs, two global cellular responses are essential for cell survival: activation of the DNA repair machinery and delay or arrest of cell cycle progression. Recently, gene expression inventories have been collected that focus on the transcriptional changes in response to different types of DNA stress (Culligan et al., 2006; Ricaud et al., 2007; Yoshiyama et al., 2009; Cools et al., 2010). To identify novel key signaling components that contribute to cell cycle checkpoint activation, we compared bleomycin-induced genes to those induced by HU treatment (Cools et al., 2010) and γ-radiation (Culligan et al., 2006; Yoshiyama et al., 2009). Twenty-two genes were upregulated in all DNA stress experiments and can be considered as transcriptional hallmarks of the DNA damage response, regardless of the type of DNA stress (Figure 1, Table 1). Within this selection, genes known to be involved in DNA stress and DNA repair are predominantly present, including *POLY(ADP-RIBOSE) POLYMERASE2* (*PARP2*), *BREAST CANCER SUSCEPTIBILITY1* (*BRCA1*), and *RAS-ASSOCIATED WITH DIABETES PROTEIN51*.

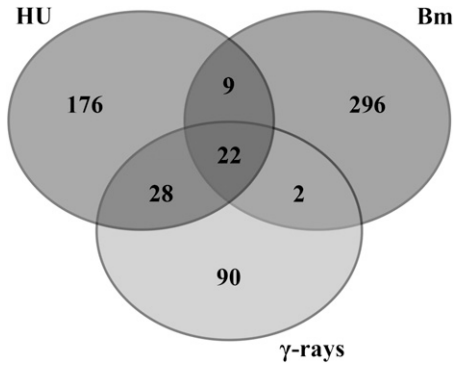

Figure 1. DNA Stress Meta-Analysis.

Venn diagram showing the overlap between transcripts induced by HU, bleomycin (Bm), and γ-radiation (γ-rays). In total, 61 genes were positively regulated in at least two DNA stress experiments and 22 genes accumulated in all DNA stress experiments.

Table 1. Overview of the Transcriptionally Induced Core DNA Damage Genes

AGI Locus[a]	Annotation	HU 24 h/0 h[b]	γ-Rays 1[c]	γ-Rays 2[d]	Bleomycin
AT4G21070	Breast cancer susceptibility1	10.375	581.570	57.803	2.386
AT5G60250	Zinc finger (C3HC4-type RING finger) family protein	8.907	34.918	40.000	2.352
AT1G07500	Siamese-related 5	7.863	38.160	35.842	1.595
AT4G02390	Poly(ADP-Rib) polymerase	7.701	131.865	59.172	2.663
AT3G07800	Thymidine kinase	7.160	46.179	20.492	2.759
AT5G03780	TRF-like 10	7.111	108.316	23.474	1.600
AT5G64060	NAC domain containing protein 103	5.579	28.086	13.755	2.153
AT2G18600	Ubiquitin-conjugating enzyme family protein	5.521	21.462	11.481	1.972
AT4G22960	Unknown function (DUF544)	5.315	36.380	14.451	2.282
AT5G48720	X-ray induced transcript 1	5.296	285.166	65.789	2.228
AT5G24280	γ-Irradiation and mitomycin c induced 1	4.823	108.578	42.918	2.584
AT5G20850	RAS associated with diabetes protein 51	4.643	186.456	31.250	1.765
AT3G27060	Ferritin/ribonucleotide reductase-like family protein	4.595	37.351	8.741	1.970
AT2G46610	RNA binding (RRM/RBD/RNP motifs) family protein	3.593	19.913	7.331	1.546
AT5G40840	Rad21/Rec8-like family protein	3.375	113.919	27.473	1.692
AT1G13330	Hop2 homolog	2.949	17.349	13.495	1.580
AT5G66130	RADIATION SENSITIVE17	2.888	30.411	10.384	1.627
AT1G17460	TRF-like 3	2.378	18.925	10.661	1.681
AT2G45460	SMAD/FHA domain-containing protein	2.378	45.673	21.053	1.575
AT5G49480	Ca^{2+} binding protein 1	1.952	15.106	5.851	1.580
AT3G25250	AGC (cAMP-dependent, cGMP-dependent, and protein kinase C) kinase family protein	1.853	12.995	17.794	1.517
AT5G55490	Gamete expressed protein 1	1.670	71.489	34.722	2.407

[a]AGI, Arabidopsis Genome Initiative.
[b]According to Cools et al. (2011).
[c]According to Culligan et al. (2006).
[d]According to Yoshiyama et al. (2009).

In addition, we recognized one member of the *SIM*/*SMR* gene family, *SMR5*. When expanding the selection by considering genes induced in at least two of the three DNA stress experiments, we identified a total of 61 genes (Supplemental Data Set 1). Besides DNA damage response–related genes, this expanded data set included an additional *SMR* family member (*SMR4*), which was expressed upon HU treatment and γ-radiation.

The *SMR* Gene Family Comprises 14 Family Members That Respond to Different Stresses

Previously, we reported on the existence of one *SIM* and five *SMR* genes (*SMR1-SMR5*) in the *Arabidopsis* genome (Peres et al., 2007), whereas protein purification of CDK/cyclin complexes resulted in the identification of two additional family members (*SMR6* and *SMR8*) (Van Leene et al., 2010). With the availability of newly sequenced plant genomes, we reexamined the *Arabidopsis* genome using iterative BLAST searches for the presence of additional *SMR* genes, resulting in the identification of six nonannotated family members, named *SMR7* to *SMR13* (Supplemental Table 1). With the Genevestigator toolbox (Hruz et al., 2008), the expression pattern of the 12 *SIM*/*SMR* genes represented on the Affymetrix ATH1 microarray platform was analyzed in response to different biotic and abiotic stress treatments. Distinct family members were induced under various stress conditions, albeit with different specificity (Figure 2). Every *SMR* gene appeared to be transcriptionally active under at least a number of stress conditions, with *SMR5* responding to most diverse types of abiotic stresses. In response to DNA stress (genotoxic stress and UV-B light treatment), two *SMR* genes responded strongly, namely, *SMR4* and *SMR5*, corresponding with their presence among the DNA stress genes identified by our microarray meta-analysis.

To confirm their involvement in the genotoxic stress response, transcriptional reporter lines containing the putative upstream promoter sequences were constructed for all *SIM*/*SMR* genes. After selection of representative reporter lines, 1-week-old seedlings were transferred to control medium or medium supplemented with HU (resulting in stalled replication forks) or bleomycin (causing DSBs). Focusing on the root tips revealed distinct expression patterns (Figure 3; Supplemental Figure 1), with some family members being restricted to the root elongation zone (including *SIM* and *SMR1*), while others were confined to vascular tissue (e.g., *SMR2* and *SMR8*) or columella cells (e.g., *SMR5*). When plants were exposed to HU, three *SMR* genes showed transcriptional induction in the root meristem, namely, *SMR4*, *SMR5*, and *SMR7*, with the latter two displaying the strongest response (Figure 3). In the presence of bleomycin, an additional weak cell-specific induction of *SMR6* was observed (Supplemental Figure 1). Transcriptional induction of *SMR4*, *SMR5*, and *SMR7* by HU and bleomycin was confirmed by quantitative RT-PCR experiments (Supplemental Figure 2). These data fit the above-described microarray analysis, with the lack of *SMR7* being explained by its absence on the ATH1 microarray of the HU and γ-irradiation

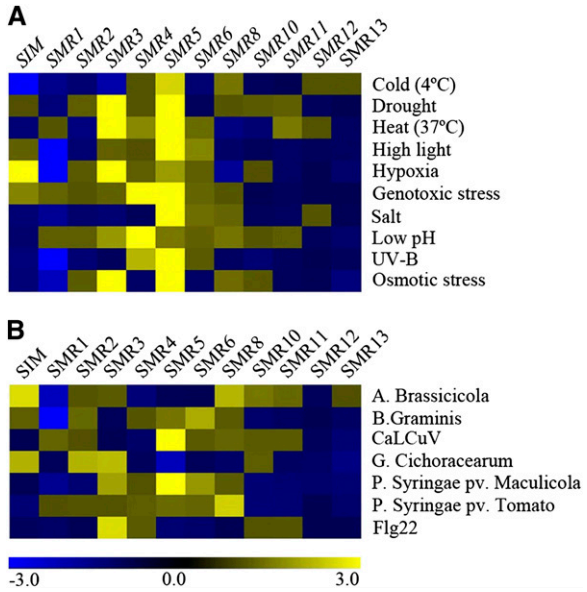

Figure 2. Hierarchical Average Linkage Clustering of *SIM*/*SMR* Genes Induced in Response to Different Stresses.

Arabidopsis plants were exposed to abiotic **(A)** and biotic **(B)** stresses. Data comprise the *SIM*/*SMR* represented in publicly available Affymetrix ATH1 microarrays obtained with the Genevestigator toolbox. Blue and yellow indicate down- and upregulation, respectively, whereas black indicates no change in expression. Values indicate fold-change in expression level in stress versus control experiments.

experiments, although being induced 5.68-fold in the bleomycin experiment performed using the Aragene array. In addition to HU and bleomycin, we confirmed the transcriptional activation of *SMR4*, *SMR5*, and *SMR7* by γ-irradiation (Supplemental Figure 3).

DNA Stress–Induced *SMR* Genes Encode Potent Cell Cycle Inhibitors

SIM had been proven to encode a potent cell cycle inhibitor, since its ectopic expression results in dwarf plants with fewer cells than control plants (Churchman et al., 2006). To test whether the DNA stress–induced *SMR* genes encode proteins with cell division inhibitory activity, *SMR4*-, *SMR5*-, and *SMR7*-overexpressing (*SMR4*^{OE}, *SMR5*^{OE}, and *SMR7*^{OE}) plants were generated. For each gene, multiple lines with high transcript levels were isolated, all showing a reduction in rosette size compared with wild-type plants (Figures 4A to 4D). This decrease in leaf size correlated with an increase in cell size (Figures 4E to 4H), indicative of a strong inhibition of cell division. Similar to *SIM* (Churchman et al., 2006), ectopic expression not only inhibited cell division but also triggered an increase in DNA content by stimulating endoreplication (Figures 4I to 4L; Supplemental Table 2), likely representing a premature onset of cell differentiation. Together with the previously described biochemical interaction between SMR4 and SMR5, and CDKA;1 and D-type cyclins (Van Leene et al., 2010), it can be concluded that the DNA stress–induced *SMR* genes encode potent cell cycle inhibitors.

SMR5 and *SMR7* Regulate a HU-Dependent Checkpoint in Leaves

To address the role of the different *SMR* genes in DNA stress checkpoint regulation, the growth response to HU treatment of plants silenced for *SMR5* or *SMR7* (Supplemental Figure 4) was

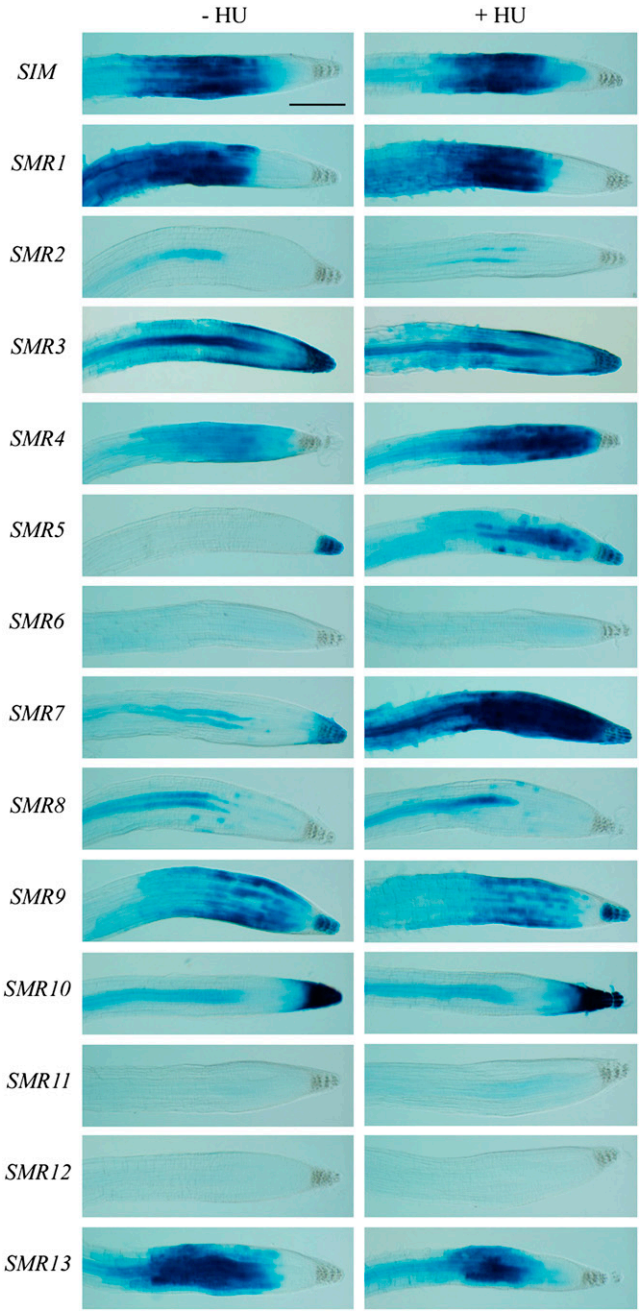

Figure 3. *SIM*/*SMR* Induction in Response to HU.

One-week-old *SMR* reporter seedlings (names indicated on the left) were transferred to control (−HU) medium or medium supplemented with 1 mM HU (+HU). GUS assays were performed 24 h after transfer. All images are at the same magnification. Bar = 200 μm.

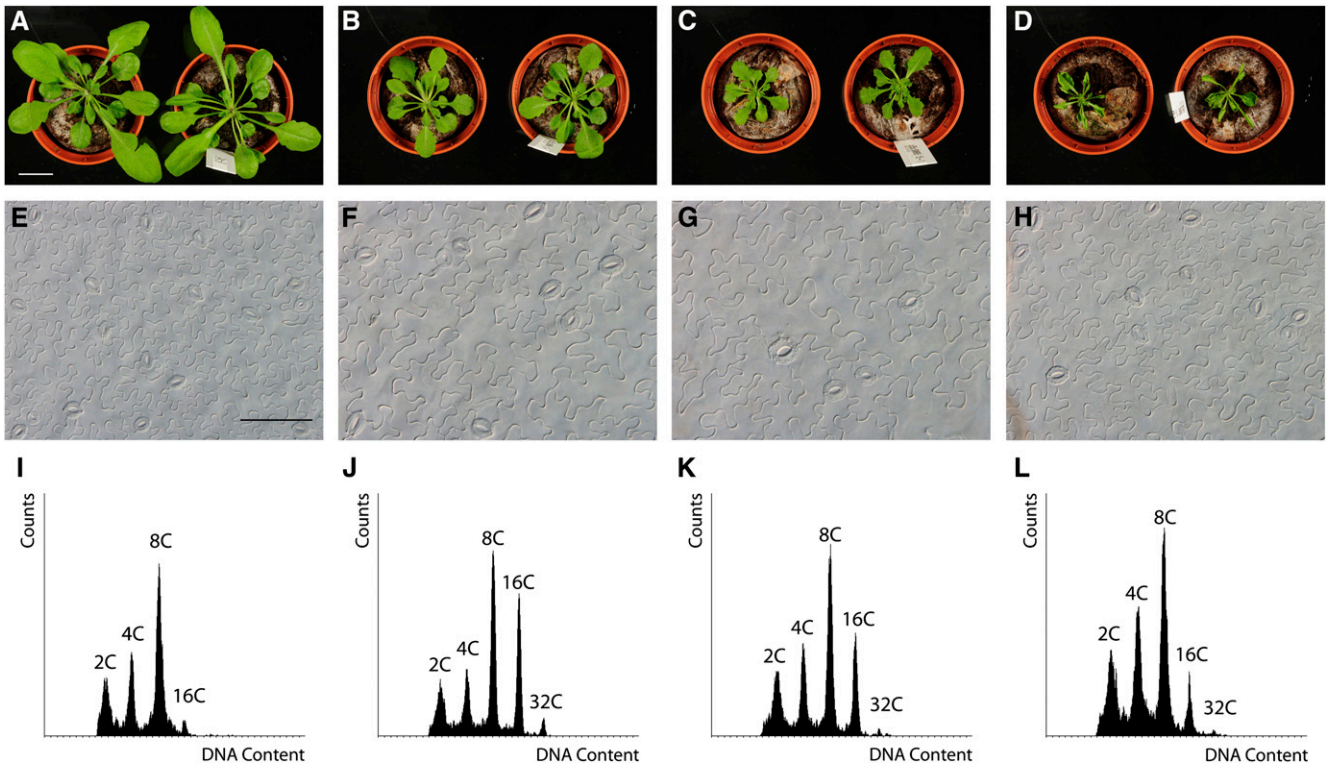

Figure 4. Ectopic *SMR4*, *SMR5*, and *SMR7* Expression Inhibits Cell Division.

(A) to **(D)** Four-week-old rosettes of control **(A)**, *SMR4*^{OE} **(B)**, *SMR5*^{OE} **(C)**, and *SMR7*^{OE} **(D)** plants. All images are at the same magnification. Bar = 2 cm.
(E) to **(H)** Leaf abaxial epidermal cell images of in vitro–grown 3-week-old control **(E)**, *SMR4*^{OE} **(F)**, *SMR5*^{OE} **(G)**, and *SMR7*^{OE} **(H)** plants. All images are at the same magnification. Bar = 100 μm.
(I) to **(L)** Ploidy level distribution of the first leaves of 3-week-old in vitro–grown control **(I)**, *SMR4*^{OE} **(J)**, *SMR5*^{OE} **(K)**, and *SMR7*^{OE} **(L)** plants.

compared with that of control plants (Columbia-0 [Col-0]). No significant difference in leaf size was observed for plants grown under standard conditions. By contrast, when comparing plants grown for 3 weeks in the presence of HU, the leaves of the knockout plants *SMR5*^{KO} and *SMR7*^{KO} were significantly larger than that of the control plants (Figure 5A). This difference was attributed to a difference in cell number. Control plants responded to the HU treatment with a 47% reduction in epidermal cell number, reflecting an activation of a stringent cell cycle checkpoint. By contrast, in *SMR5*^{KO} and *SMR7*^{KO} plants this reduction was restricted to 29 and 30%, respectively (Figure 5B). Within the *SMR5*^{KO} *SMR7*^{KO} double mutant, the reduction in leaf size and cell number was even less (Figures 5A and 5B), suggesting that both inhibitors contribute to the cell cycle arrest observed in the control plants by checkpoint activation upon HU stress. A similar role of SMR4 could not be tested due to the lack of an available knockout.

SMR5 and *SMR7* Expression Is Triggered by Oxidative Stress

Because of the observed role of *SMR5* and *SMR7* in DNA stress checkpoint regulation, we analyzed the dependence of their expression on the ATM and ATR signaling kinases and the SOG1 transcription factor by introducing the *SMR5* and *SMR7* β-glucuronidase (GUS) reporter lines into the *atr-2*, *atm-1*, and *sog1-1* mutant backgrounds. Both genes were induced in the proliferating leaf upon HU and bleomycin treatment (Figure 6). Moreover, as would be expected for a DSB-inducing agent, the transcriptional activation of *SMR5* and *SMR7* by bleomycin depended on ATM and SOG1. Surprisingly, the same pattern was observed for HU, whereas one would expect that *SMR5*/*SMR7* induction after arrest of the replication fork would rely on ATR-dependent signaling. These data indicate that the HU-dependent activation of *SMR5* and *SMR7* might be caused by a genotoxic effect of HU being unrelated to replication stress induced by the depletion of dNTPs. A recent study demonstrated that HU directly inhibits catalase-mediated H_2O_2 decomposition (Juul et al., 2010). Analogously, in combination with H_2O_2, HU has been demonstrated to act as a suicide inhibitor of ascorbate peroxidase (Chen and Asada, 1990). Combined, both mechanisms are likely responsible for an increase in the cellular H_2O_2 concentration, which might trigger DNA damage and, consequently, transcriptional induction of the *SMR5* and *SMR7* genes. Indeed, extracts of control plants treated with HU displayed a reduced H_2O_2 decomposition rate (Figure 7A). As catalase and ascorbate peroxidase activity are essential for the scavenging of H_2O_2 that is generated upon high-light exposure,

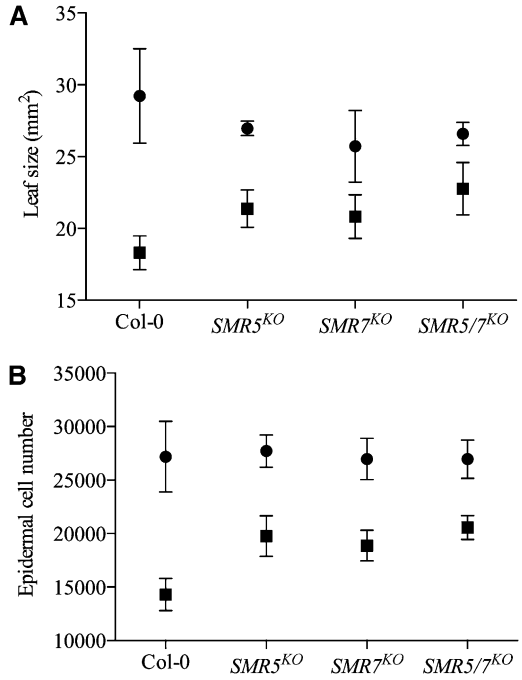

Figure 5. SMR5 and SMR7 Are Required for an HU-Dependent Cell Cycle Checkpoint.

Leaf **s**ize **(A)** and abaxial epidermal cell number **(B)** of the first leaves of 3-week-old plants grown on control medium (circles) or medium supplemented with 1 mM HU (squares). Data represent mean with 95% confidence interval (two-way ANOVA, $n = 10$).

we subsequently tested the effects of HU treatment on photosystem II (PSII) efficiency in 1-week-old seedlings after transfer from low- to high-light conditions. As illustrated in Figure 7B, transfer for 48 h to high light resulted in a decrease of maximum quantum efficiency of PSII. In the presence of HU, the maximum quantum efficiency of PSII decrease was even more pronounced, which again corroborates the idea that HU might interfere with H_2O_2 scavenging. Macroscopically, plants grown in the presence of HU showed visible anthocyanin pigmentation in the young leaf tissue within 48 h after transfer, whereas plants grown on control medium showed no effect of the transfer to high light (Figure 7C).

To examine whether an increase in H_2O_2 might trigger expression of *SMR* genes, *SMR5* and *SMR7* expression levels were analyzed in plants that are silenced for *CAT2* and/or *APX1*, encoding two enzymes important for H_2O_2 scavenging. Whereas *SMR5* transcript levels appeared to be stable over all genotypes, *SMR7* expression levels were clearly induced in the single *apx1* and *apx1 cat2* double mutant (Figure 8A). As an independent strategy to induce ROS, *SMR5* and *SMR7* GUS reporter lines were transferred from control (70 to 80 μmol m^{-2} s^{-1}) to high light (300 to 400 μmol m^{-2} s^{-1}) conditions for 2 d. Whereas *PSMR7:GUS* plants displayed an increase in GUS activity being mainly restricted to the shoot apex, *SMR5* promoter activity was strongly stimulated in both the shoot apex and leaf tissue (Figure 8B). *SMR5* induction under high light was confirmed by RT-PCR (Supplemental Figure 5). To examine whether this transcriptional induction contributed to a high-light-induced cell cycle checkpoint, we measured epidermal cell numbers in mature first leaves of control (Col-0), *SMR5*^{KO}, and *SMR7*^{KO} plants that were transferred for 4 d to high-light conditions at a period when their leaf cells were still undergoing cell division. This high light treatment resulted into a 34 and 38% reduction in cell number in control and *SMR7*^{KO} plants, respectively (Figure 8C). By contrast, *SMR5*^{KO} plants displayed only a 13% reduction in cell number, illustrating that SMR5 is essential to activate a high-light-dependent cell cycle checkpoint.

SMR5 and *SMR7* Are under Direct Regulation of SOG1

Recently, it was found that the SOG1 transcription factor becomes hyperphosphorylated in an ATM-dependent manner upon the occurrence of DSBs, such as induced by γ-irradiation or treatment with the radiomimetic drug zeocin, and that this phosphorylation is essential for SOG1 activity (Yoshiyama et al., 2013). As *SMR5* and *SMR7* transcription was found to depend on SOG1 and because both *SMR* genes respond to oxidative stress, we tested whether SOG1 phosphorylation occurs in response to H_2O_2 treatment. Lines expressing a Myc-tagged *SOG1* under the control of its own promoter (*PSOG1:SOG1-Myc*) were either transferred to control medium or medium supplemented with H_2O_2. As described previously, immunoblotting using anti-Myc antibody detected two bands under control conditions (Figure 9A), with the upper band corresponding to SOG1 phosphorylated in a DNA stress–independent manner by a yet to be identified kinase (Yoshiyama et al., 2013). Upon H_2O_2 treatment, a third slowly migrating band appeared at a similar position as detected by zeocin treatment (Yoshiyama et al., 2013). This band disappeared when protein extracts were treated with the λ protein phosphatase (λPP), indicating that it corresponds to a phosphorylated form of SOG1 (Figure 9A).

Subsequently, as *SMR5* and *SMR7* transcription was found to depend on SOG1 (Figure 6), we tested whether both genes are under the direct control of SOG1. Direct binding of SOG1 to the *SMR5* and *SMR7* promoters was tested through chromatin immunoprecipitation (ChIP) using *PSOG1:SOG1-Myc* seedlings that were either transferred to control medium or medium supplemented with the DSB-inducing drug zeocin for 2 h. Promoter scanning revealed that SOG1 binds in a DNA stress–dependent manner to both *SMR* promoters in close proximity to their transcription start sites (Figures 9B and 9C). These data illustrate that both *SMR* genes are under direct control of SOG1.

DISCUSSION

At Least Two Different Functional SMR Groups Exist

In this work, we analyzed the SIM/SMR group of CKIs. All share only limited sequence homology, being restricted to short amino acid regions scattered along the protein sequences, among which is a 6–amino acid domain corresponding to a cyclin binding motif (Peres et al., 2007). Although this poor sequence alignment does not allow a clear phylogenetic analysis, biochemically it appears that SIM/SMR proteins fall into at least two different

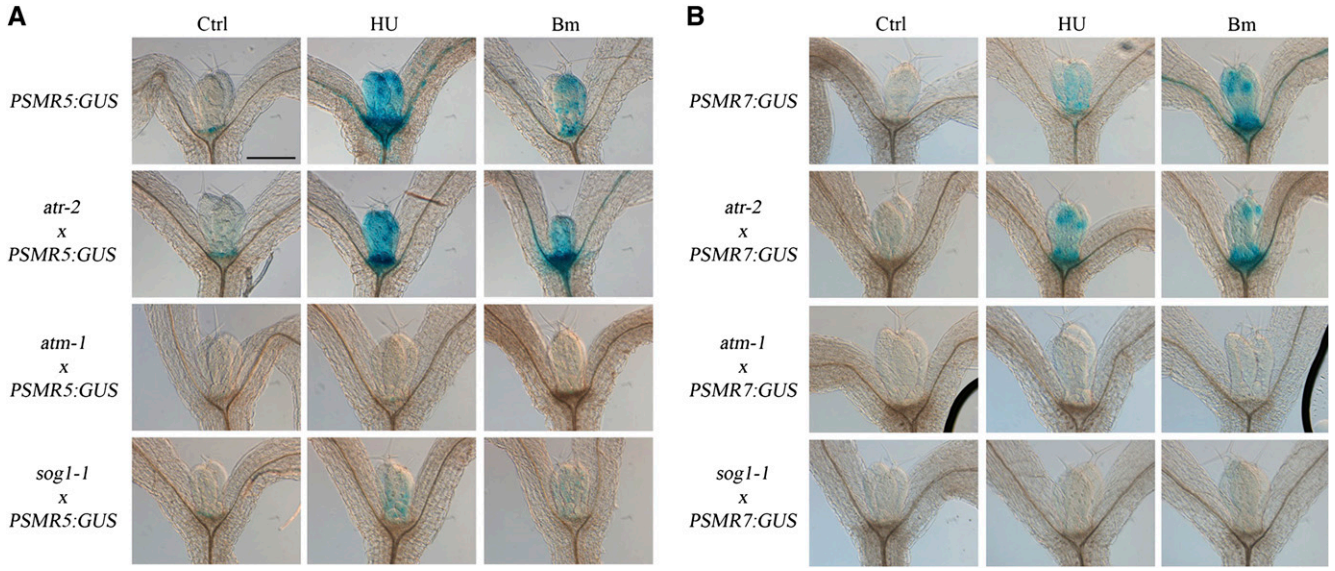

Figure 6. *SMR5* and *SMR7* Expression Is ATM and SOG1 Dependent.

PSMR5:GUS **(A)** and *PSMR7:GUS* **(B)** reporter constructs introgressed into *atr-2*, *atm-1*, and *sog-1* mutant backgrounds were transferred to control medium (Ctrl) or medium supplemented with 2 mM HU or 0.3 μg/mL bleomycin (Bm) for 24 h. All images are at the same magnification. Bar = 250 μm.

categories. The first category includes the founding members SIM and SMR1 that both have been linked to endocycle onset (Churchman et al., 2006; Roeder et al., 2010), being an alternative cell cycle in which mitosis is repressed in favor of repetitive rounds of DNA replication, resulting in an increase in DNA ploidy level. Through protein purification, these two SMRs were found to copurify with the B-type CDKB1;1 (Van Leene et al., 2010), in agreement with the observation that this particular CDK needs to be inhibited for endocycle onset (Boudolf et al., 2004, 2009). A role in endocycle onset is supported by their expression pattern in the root, showing specific transcription in the cell elongation zone, likely representing the zone of cells in which endocycling begins. In addition to SIM and SMR1, SMR2 also exclusively copurifies with CDKB1;1, suggesting that this particular CKI might also be an SMR family member linked with endocycle onset. As a second category, other SMRs, including SMR4 and SMR5, exclusively copurify with the A-type CDK and D-type cyclins (Van Leene et al., 2010). CDKA;1 is the main driver of S-phase progression (Nowack et al., 2010, 2012), whereas the CYCD/CDKA;1 complex regulates cell cycle onset in response to intrinsic and extrinsic signals (Riou-Khamlichi et al., 2000; Dewitte and Murray, 2003). Therefore, CYCD/CDKA;1 appears to be the most logical CYC/CDK complex to be targeted by those SMRs that aim to link DNA stress signals with cell cycle checkpoint activation.

HU Affects DNA Integrity in Multiple Ways

HU is known for its inhibitory effect on RNR activity, resulting in the depletion of the available dNTPs, causing impaired progression of the replication fork and activation of an ATR-dependent replication checkpoint. However, the observed ATM-dependent induction of *SMR5* and *SMR7* upon HU treatment suggests that HU affects DNA integrity also in an RNR-independent manner. In particular, our data indicate that ROS might be the primary trigger of *SMR5* and *SMR7* expression upon HU treatment. A link between HU and oxidative stress has been observed previously in *Saccharomyces cerevisiae*, where, besides a DNA replication arrest caused by RNR inhibition, exposure to HU results in the activation of the Yap regulon that reacts to oxidative stress and encompasses genes involved in cellular redox homeostasis (Dubacq et al., 2006). In *Arabidopsis*, Juul et al. (2010) reported a direct interaction between HU and catalase, resulting in a stereoinhibition of the detoxifying capabilities of the catalase protein. Analogously, HU was demonstrated to be a suicide inhibitor of ascorbate peroxidase (Chen and Asada, 1990). In agreement, we demonstrated that HU treatment results in a decrease in the H_2O_2 scavenging rate. A second source of HU-induced ROS might originate from displacement of the essential cofactor iron from the RNR catalytic site (Nyholm et al., 1993), probably resulting in an increase in the intracellular iron concentration. This increase might contribute to the increase in ROS, as iron catalyzes the production of hydroxyl radicals from H_2O_2 through the Fenton reaction. Together, the increased H_2O_2 and iron levels after HU treatment represent a potent source of oxidative stress. The HU-induced oxidative state results in the accumulation of anthocyanin pigments and the reduction in PSII efficiency. The latter is likely due to the deceleration of PSII repair, consequently resulting in further increased levels of intracellular ROS and enhanced photoinhibition (Murata et al., 2012).

Because of its relatively long life and permeability, H_2O_2 is able to migrate into different cellular compartments. Besides PSII inhibition, H_2O_2 and hydroxyl radicals are known to affect the DNA in multiple ways, including the oxidation of bases, the creation of DNA interstrand cross-links, and DSBs (Cadet et al.,

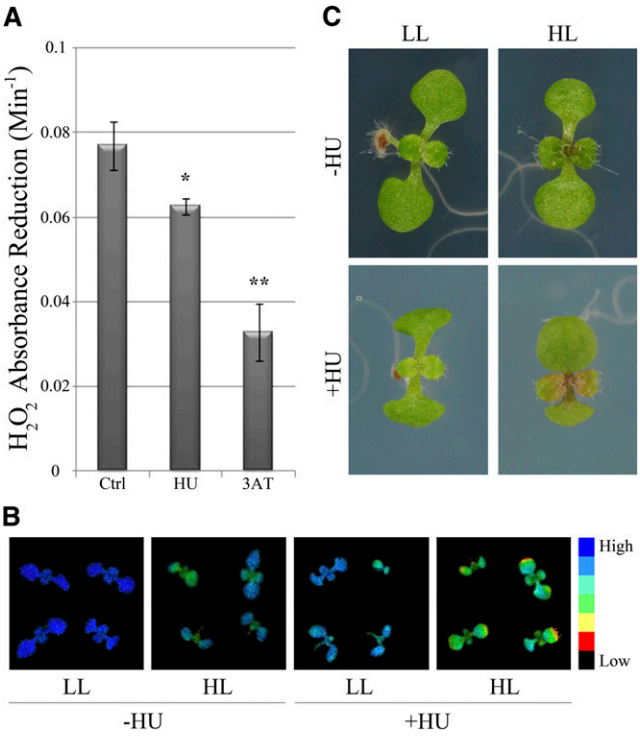

Figure 7. HU Triggers Oxidative Stress.

(A) H_2O_2 scavenging in extracts from 1-week-old untreated control (Ctrl), HU-treated (1 mM), and 3-amino-1,2,4-triazole (3AT)–treated (6 μM) (positive control) plants. Error bars show SE (n = 3 to 4). *P value < 0.05; **P value < 0.01 (two-tailed Student's t test).

(B) Fluorescence images displaying maximum quantum efficiency of PSII of 6-d-old seedlings grown under low (LL) and high (HL) light for 48 h in the absence (−HU) and presence (+HU) of 1 mM HU.

(C) Light microscope images of plants shown in **(B)**.

2012), triggering ATM-dependent signaling. In mammals, oxidation of ATM directly induces its activation (Guo et al., 2010); however, whether a similar mechanism is functional in plants is unknown. In agreement with H_2O_2 acting as a putative DNA stress–inducing compound, it has been reported that the lack of both catalase and cytosolic ascorbate peroxidase activity results in the transcriptional activation of DNA stress genes, including *PARP2* and *BRCA1* (Vanderauwera et al., 2011). The fact that within these *apx1 cat2* double mutants no detectable rise in ROS levels could be measured suggests that experimentally undetectable levels of H_2O_2 can already trigger a DNA damage response. Interestingly, the resulting constitutive DNA damage response of the *apx1 cat2* plant grants them enhanced tolerance to DNA stress–inducing conditions.

SMR5 and *SMR7* Respond to ROS-Induced DNA Damage

Expression analysis under different ROS accumulating conditions strongly indicates that the transcriptional activation of *SMR5* and *SMR7* in response to HU is primarily mediated through changes in ROS homeostasis rather than by replication stress. Interestingly, *SMR5* and *SMR7* appear to display a differential transcriptional response toward distinct sources of ROS. Under high-light treatment, which likely generates singlet oxygen rather than H_2O_2 (Mittler, 2002), it is mainly *SMR5* that is induced, in agreement with the observation that a high-light-induced cell cycle checkpoint was only abrogated in the *SMR5*^{KO} plants. By contrast, *SMR7* is the main gene induced in the *apx1* and *apx1 cat2* mutants. Similar to mature *apx1 cat2* double mutant plants, young *apx1* mutants display an activated DNA stress response, as supported by the elevated expression of DNA damage reporter

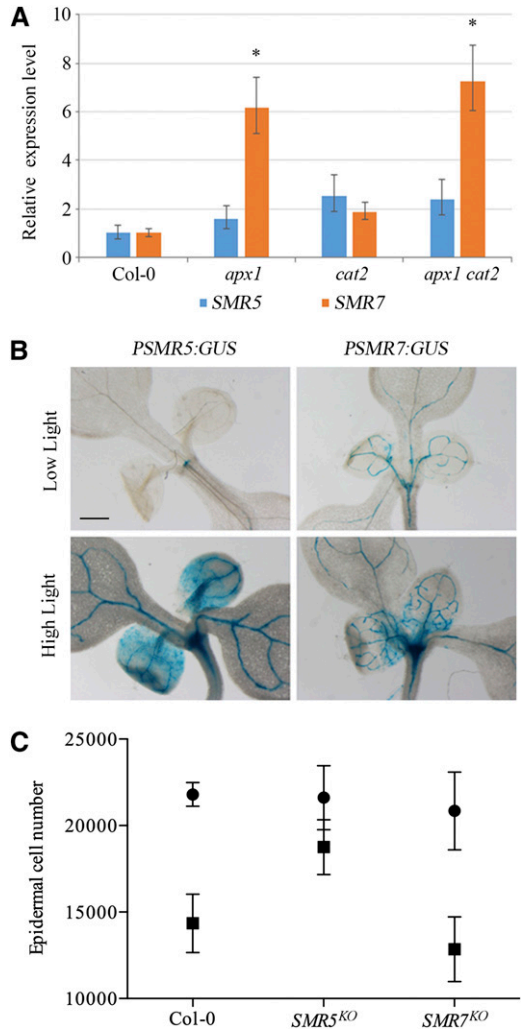

Figure 8. *SMR5* and *SMR7* Are Induced by Oxidative Stress–Inducing Stimuli.

(A) Relative *SMR5* and *SMR7* expression levels in shoots of 6-d-old wild-type (Col-0), *apx1*, *cat2*, and *apx cat2* mutant plants. Data represent least square means ± SE, normalized to wild-type levels that were arbitrary set to one (n = 3, *P value < 0.01).

(B) One-week-old *PSMR5:GUS* and *PSMR7:GUS* seedlings grown under low- versus high-light conditions for 48 h. All images are at the same magnification. Bar = 500 μm.

(C) Abaxial epidermal cell number of the first leaves of 3-week-old plants transferred at the age of 8 d for 96 h to control (circles) or high-light (squares) conditions. Data represent mean with 95% confidence interval (two-way ANOVA, n = 8).

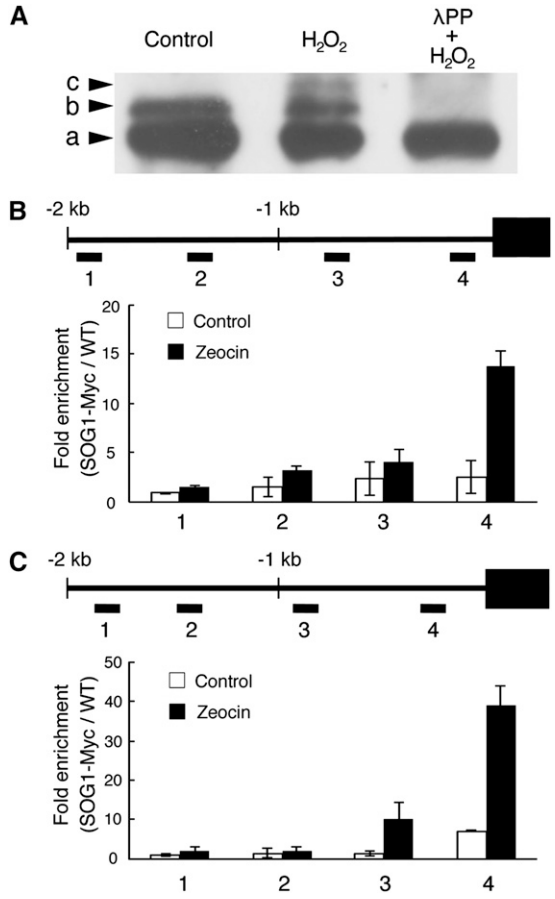

Figure 9. In Vivo Phosphorylation of SOG1 by H_2O_2 and Its Association with the *SMR5* and *SMR7* Promoters.

(A) Total protein was immunoblotted with anti-Myc antibody. Plants harboring *PSOG1:SOG1-Myc* were treated with or without H_2O_2, and total protein was extracted. Total protein from H_2O_2-treated plants was incubated with λPP. The phosphorylated forms of SOG1 were separated in an SDS-PAGE gel containing Phos-tag. Nonphosphorylated, phosphorylated, and hyperphosphorylated SOG1-Myc (bands a, b, and c, respectively) are indicated by arrowheads.

(B) and **(C)** Chromatin bound to the promoter regions of *SMR5* **(B)** and *SMR7* **(C)** was collected by immunoprecipitation with anti-Myc antibodies from *PSOG1:SOG1-MYC* plants treated with (black bars) and without (white bars) 15 μM zeocin and subjected to qPCR analysis. Fold enrichment for each DNA fragment was determined by dividing the recovery rate with that of wild-type plants (WT = 1). Bar graphs represent the average of two biological replicate ChIP experiments ± SE. Positions of PCR amplicons 1 to 4 are also shown.

genes under control conditions in 8-d-old seedlings (see Supplemental Figure 2 in Vanderauwera et al., 2011). This constitutive DNA damage response likely results from H_2O_2 leaking from the chloroplast (Davletova et al., 2005) and reaching the nucleus in the absence of cytosolic scavenging by APX1. The mechanisms by which different *SMR* genes respond to different types of ROS are currently unknown.

From our data, it can be concluded that HU simultaneously triggers two different cell cycle checkpoint cascades: one related to replication stress and one that responds to H_2O_2, regulated by ATR and ATM, respectively (Figure 10). Roots of plants silenced for the replication stress checkpoint activators *ATR* or *WEE1* are hypersensitive to HU, indicating that the HU-induced replication defect prevails in roots. By contrast, despite their transcriptional induction, no clear root phenotype was observed for the $SMR5^{KO}$ and $SMR7^{KO}$ plants (Supplemental Figure 6). The restriction of a HU-sensitive phenotype to tissues with photosynthetic activity therefore suggests that the primary response of HU in the shoot tissue might be ROS accumulation (Figure 10). Remarkably, our data indicate that the signaling pathway by which oxidative stress induces *SMR5*/*SMR7* expression is relatively short, with ATM phosphorylating the SOG1 transcription factor that binds directly to the *SMR* promoters to activate their transcription, as supported by the observation that no *SMR5*/*SMR7* expression is observed in the *sog1-1* mutant background. Because SOG1 only associates with the *SMR5* and *SMR7* promoters in the samples in which DNA stress was induced, we speculate that phosphorylation of SOG1 is a prerequisite for binding to its target genes.

In addition to being induced by genotoxic stress, *SMR5* displays a strong transcriptional response to many different abiotic stress conditions that also involve ROS signaling, including drought, high light, and salt (Figure 2). Therefore, SMR5 might be a general integrator of ROS signaling with cell cycle progression. ROS signaling has previously been linked to cell cycle progression. Treatment of tobacco cells with a ROS-inducing agent impairs the G1-to-S transition, retards the S-phase progression, and delays entry into M-phase, in correlation with the downregulation of CDK activity (Reichheld et al., 1999). Moreover, it has been demonstrated that the G1-to-S transition requires

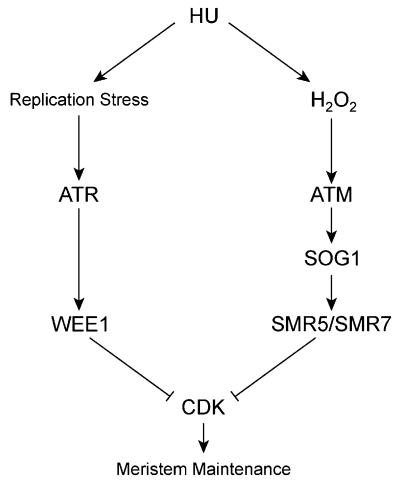

Figure 10. Model for HU-Dependent Cell Cycle Checkpoint Activation.

HU treatment results in replication stress and an increase in the cellular H_2O_2 concentration, likely resulting in DNA damage that is sensed by the ATR and ATM signaling cascades, respectively. ATR activates a checkpoint response through transcriptional induction of *WEE1*, whereas ATM does the same through activation of *SMR5* and *SMR7*. Both pathways allow cells to adapt to the DNA stress and thereby contribute to meristem maintenance.

adequate levels of the antioxidant glutathione. Accordingly, the *ROOT MERISTEMLESS1* gene, encoding a glutathione biosynthetic enzyme, is required to establish an active meristem (Vernoux et al., 2000). Additionally, recent evidence indicates that the distribution of ROS regulates the transition from proliferation to differentiation: The basic helix-loop-helix transcription factor UPBEAT1 (UPB1) is expressed at the root transition zone and regulates the distribution of ROS by monitoring the expression level of peroxidase genes (Tsukagoshi et al., 2010). Strikingly, the same study revealed that the *SIM* promoter is bound by the UPB1 protein, which is in agreement with our observation that *SIM* expression is restricted to the root elongation zone, which is also the site of maximum H_2O_2 concentration (Dunand et al., 2007). Likewise, ROS signaling has been implicated in pathogen response, whereas the first rice *SIM*/*SMR*-like gene (*EL2*) was described originally as a gene being induced within minutes after addition of the elicitor *N*-acetylchitoheptaose or purified flagellin protein of the pathogen *P. Avenae I* (Minami et al., 1996; Che et al., 2000). Moreover, H_2O_2 has also been detected in root columella cells, root cap cells, and vascular cells (Dunand et al., 2007; Tsukagoshi et al., 2010), to which specific *SMR* expression patterns can be linked. These data suggest that the transcriptional activation of *SIM*/*SMR* genes in response to ROS signals might be a general mechanism linking the oxidative status of a cell with its cell division activity.

METHODS

Plant Materials and Growth Conditions

The *smr5* (SALK_100918) and *smr7* (SALK_128496) alleles were acquired from the ABRC. Homozygous insertion alleles were checked by genotyping PCR using the primers listed in Supplemental Table 3. The *atm-1*, *atr-2*, and *sog1-1* mutants have been described previously (Garcia et al., 2003; Preuss and Britt, 2003; Culligan et al., 2004; Yoshiyama et al., 2009). Unless stated otherwise, plants of *Arabidopsis thaliana* (ecotype Columbia) were grown under long-day conditions (16 h of light/8 h of darkness) at 22°C on half-strength Murashige and Skoog (MS) germination medium (Murashige and Skoog, 1962). *Arabidopsis* plants were treated with HU as described by Cools et al. (2011). For bleomycin treatments, 5-d-old seedlings were transferred into liquid MS medium supplemented with 0.3 μg/mL bleomycin. For γ-irradiation treatments, 5-d-old in vitro–grown plantlets were irradiated with γ-rays at a dose of 20 Gy. For light treatments, 1-week-old seedlings were transferred to continuous high-light conditions (growth rooms kept at 22°C with 24-h day/0-h night cycles and a light intensity of 300 to 400 μmol m^{-2} s^{-1}) for 4 d and subsequently retransferred to low-light conditions (70 to 80 μmol m^{-2} s^{-1}).

DNA and RNA Manipulation

Genomic DNA was extracted from *Arabidopsis* leaves with the DNeasy plant kit (Qiagen), and RNA was extracted from *Arabidopsis* tissues with the RNeasy mini kit (Qiagen). After DNase treatment with the RQ1 RNase-Free DNase (Promega), cDNA was synthesized with the iScript cDNA synthesis kit (Bio-Rad). Quantitative RT-PCR was performed using the SYBR Green kit (Roche) with 100 nM primers and 0.125 μL of RT reaction product in a total volume of 5 μL per reaction. Reactions were run and analyzed on the LightCycler 480 (Roche) according to the manufacturer's instructions with the use of the following reference genes for normalization: *ACTIN2*, *EMB2386*, *PAC1*, and *RPS2*6C. Primers used for the RT-PCR are given in Supplemental Table 3. Statistical analysis was executed with the Statistical Analysis Software (SAS Enterprise Guide 5.1; SAS Institute) using the mixed model procedure, and P values were Bonferroni adjusted for multiple measurements.

SIM/*SMR* promoter sequences were amplified from genomic DNA by PCR using the primers described in Supplemental Table 3. The product fragments were created with the Pfu DNA polymerase kit (Promega) and were cloned into a pDONR P4-P1r entry vector by BP recombination cloning and subsequently transferred into the pMK7S*NFm14GW,0 destination vector by LR cloning, resulting in a transcriptional fusion between the promoter of the *SMR* genes and the *nlsGFP-GUS* fusion gene (Karimi et al., 2007). For the overexpression constructs, the *SMR* coding regions were amplified using primers described in Supplemental Table 3 and cloned into the pDONR221 vector by BP recombination cloning and subsequently transferred into the pK2GW7 destination vector (Karimi et al., 2002) by LR cloning. Based on the available annotation, the amplification of the *SMR5* coding sequence yielded in a fragment of smaller size than expected, which suggested sequence misannotation. Further sequencing analysis confirmed the lack of the intronic region. The corrected coding sequencing of *SMR5* is represented in Supplemental Figure 4. All constructs were transferred into the *Agrobacterium tumefaciens* C58C1RifR strain harboring the pMP90 plasmid. The obtained *Agrobacterium* strains were used to generate stably transformed *Arabidopsis* lines with the floral dip transformation method (Clough and Bent, 1998). Transgenic plants were selected on 35 mg/L kanamycin-containing medium and later transferred to soil for optimal seed production. All cloning primers are listed in Supplemental Table 3.

GUS Assays

Complete seedlings or tissue cuttings were stained in multiwell plates (Falcon 3043; Becton Dickinson). GUS assays were performed as described by Beeckman and Engler (1994). Samples mounted in lactic acid were observed and photographed with a stereomicroscope (Olympus BX51 microscope) or with a differential interference contrast microscope (Leica).

Microscopy

For leaf measurements, first leaves were harvested at 21 d after sowing on control medium or on medium supplemented with 1 mM HU. Leaves were cleared overnight in ethanol, stored in lactic acid for microscopy, and observed with a microscope fitted with differential interference contrast optics (Leica DMLB). The total (blade) area was determined from images digitized directly with a digital camera mounted on a stereozoom microscope (Stemi SV11; Zeiss). From scanned drawing-tube images of the outlines of at least 30 cells of the abaxial epidermis located between 25 to 75% of the distance between the tip and the base of the leaf, halfway between the midrib and the leaf margin, the following parameters were determined: total area of all cells in the drawing and total numbers of pavement and guard cells, from which the average cell area was calculated. The total number of cells per leaf was estimated by dividing the leaf area by the average cell area (De Veylder et al., 2001). Leaf sizes and epidermal cell numbers in the different lines were analyzed and compared by performing a two-way ANOVA (P value < 0.05). Tukey's test was used to correct for family-wise error rate. For confocal microscopy, root meristems were analyzed 2 d after transfer using a Zeiss LSM 510 laser scanning microscope and the LSM Browser version 4.2 software (Zeiss). Plant material was incubated for 2 min in a 10 μM propidium iodide solution to stain the cell walls and was visualized with a HeNe laser through excitation at 543 nm. Green fluorescent protein (GFP) was detected with the 488-nm line of an argon laser. GFP and propidium iodide were detected simultaneously by combining the settings indicated above in the sequential scanning facility of the microscope. Acquired images were quantitatively

analyzed with ImageJ v1.45s software (http://rsbweb.nih.gov/ij/) and Cell-o-Tape plug-ins (French et al., 2012). Chlorophyll *a* fluorescence parameters were measured using the Imaging PAM M-Series chlorophyll fluorescence (Walz) and associated software.

Flow Cytometry Analysis

For flow cytometry analysis, root tip tissues were chopped with a razor blade in 300 μL of 45 mM $MgCl_2$, 30 mM sodium citrate, and 20 mM 3-morpholinopropane-1-sulfonic acid, pH 7.0 (Galbraith et al., 1991). One microliter of 4′,6-diamidino-2-phenylindole from a stock of 1 mg/mL was added to the filtered supernatant. Leaf material was chopped in 200 μL of Cystain UV Precise P nuclei extraction buffer (Partec), supplemented with 800 μL of staining buffer. The mix was filtered through a 50-μm green filter and read by the Cyflow MB flow cytometer (Partec). The nuclei were analyzed using Cyflogic software.

Catalase Assay

Plants were germinated on either control medium or medium with 1 mM HU or 6 μM 3-amino-1,2,4-triazole. Leaf tissue of 10 plants was ground in 200 μL extraction buffer (60 mM Tris, pH 6.9, 1 mM phenylmethylsulfonyl fluoride, and 10 mM DTT) on ice. The homogenate was centrifuged at 13,000*g* for 15 min at 4°C. A total of 45 μg protein extract was mixed with potassium phosphate buffer (50 mM, pH 7.0) (Vandenabeele et al., 2004). After the addition of 11.4 μL H_2O_2 (7.5%), the absorbance of the sample at 240 nm was measured over a 60-s interval to determine catalase activity (Beers and Sizer, 1952; Vandenabeele et al., 2004).

ChIP

ChIP experiments were performed as described (Gendrel et al., 2005) with minor modifications. Surface-sterile *PSOG1:SOG1-Myc* (Yoshiyama et al., 2013) seeds were germinated in 100 mL of 0.5× MS medium containing 1.5% Suc, pH 5.7, and cultured under continuous light at 23°C with gentle shaking (50 rpm). After a 14-d culture period, the seedlings were treated with 15 μM zeocin (Invitrogen) or water for 2 h. Wild-type (Col-0), no-treatment seedlings were used as a negative control. Sonicated chromatin solution (corresponding to 0.3 g tissue) was used for immunoprecipitation with anti-Myc antibodies (clone 4A6; Millipore) and an antibody recognizing an invariant domain of histone H3 (AB1791; Abcam). The ChIP products were used for quantitative PCR (qPCR) analysis with the primers listed in Supplemental Table 3. qPCR was performed with the LightCycler system (Roche) and Thunderbird SYBR qPCR Mix (Toyobo) according to the following reaction conditions: 95°C for 1 min; 70 cycles at 95°C for 10 s, at 60°C for 10 s, and at 72°C for 20 s. The signal obtained from ChIP with an anti-Myc antibody was normalized to that obtained from ChIP with an anti-Histone H3 antibody. Finally, each normalized ChIP value was divided by the normalized wild-type ChIP value to calculate the fold enrichment.

Microarray Analysis

Seeds were plated on sterilized membranes and grown under a 16-h/8-h light/dark regime at 21°C. After 2 d of germination and 5 d of growth, the membrane was transferred to MS medium containing 0.3 μg/mL bleomycin for 24 h. Triplicate batches of root meristem material were harvested for total RNA preparation using the RNeasy plant mini kit (Qiagen). Each of the different root tip RNA extracts were hybridized to 12 Affymetrix *Arabidopsis* Gene 1.0 ST arrays according to the manufacturer's instructions at the Nucleomics Core Facility. Raw data were processed with the robust multiarray algorithm (Irizarry et al., 2003) using Affymetrix Power Tools and subsequently subjected to a significance analysis of microarray analysis with MultiExperiment Viewer 4 (MeV4) of The Institute for Genome Research (Tusher et al., 2001). The imputation engine was set as 10-nearest neighbor imputer and the number of permutations was 100. Expression values were obtained by $\log_2$ transforming the average value of the normalized signal intensities of the triplicate samples. Fold changes were obtained using the expression values of the treatment relative to the control samples. Genes with Q-values < 0.1 and fold change > 1.5 or < 0.666 were retained for further analysis.

Microarray Meta-Analysis

Transcripts induced by bleomycin (Q-value < 0.1 and fold change > 1.5) were compared with different published DNA stress–related data sets. For γ-irradiation, an intersect of the genes with a significant induction (P value < 0.05, Q-value < 0.1, and fold change >1.5) in 5-d-old wild-type seedlings 1.5 h postirradiation (100 Gy) was made of two independent experiments (Culligan et al., 2006; Yoshiyama et al., 2009). For replication stress, genes were selected that showed a significant induction (P value [time] < 0.05, Q-value [time] < 0.1, and fold change >1.5) in 5-d-old wild-type root tips after 24 h of 2 mM HU treatment (Cools et al., 2011). Meta-analysis of the *SMR* genes during various stress conditions and treatments were obtained using Genevestigator (Hruz et al., 2008). Using the "Response Viewer" tool, the expression profiles of genes following different stimuli were analyzed. Only biotic and abiotic stress treatments with a more than 2-fold change in the transcription level (P value < 0.01) for at least one of the *SMR* genes were taken into account. Fold-change values were hierarchically clustered for genes and experiments by average linkage in Multiple experiment Viewer from The Arabidopsis Information Resource.

SOG1 Phosphorylation Assay

Plants harboring *PSOG1:SOG1-Myc* (Yoshiyama et al., 2013) were grown on MS media (1× MS salts including vitamins, 2% [w/v] Suc, and 0.8% [w/v] gellangum, pH 6.0) under continuous light at 23°C. Five-day-old seedlings were transferred onto new MS medium or medium supplemented with 5 mM H_2O_2 and incubated for 24 h. Total protein was extracted from roots and immunoblotted with anti-Myc antibody (Santa Cruz) as described by Yoshiyama et al. (2013). To detect phosphorylated SOG1 proteins, Phos-tag reagent (NARD Institute) was used for the phoshoprotein mobility shift assay (Kinoshita et al., 2006). λPP (New England Biolabs) was used to dephosphorylate the phosphorylated forms of SOG1.

Accession Numbers

Microarray results have been submitted to MiamExpress (www.ebi.ac.uk/miamexpress) under accession number E-MEXP-3977. Sequence data from this article can be found in the Arabidopsis Genome Initiative or GenBank/EMBL databases under the following accession numbers: *SMR4* (At5g02220), *SMR5* (At1g07500), *SMR7* (At3g27630), *ATM* (At3g48490), *ATR* (At5g40820), *SOG1* (At1g25580), *ACTIN2* (At3g46520), *EMB2386* (At1g02780), *PAC1* (At3g22110), and *RPS26C* (At3g56340).

Supplemental Data

The following materials are available in the online version of this article.

Supplemental Figure 1. *SIM*/*SMR* Induction in Response to Bleomycin.

Supplemental Figure 2. Transcriptional Induction of *SIM*/*SMR* Genes upon HU and Bleomycin Treatment.

Supplemental Figure 3. Transcriptional Induction of *SIM*/*SMR* Genes upon γ-Irradiation.

Supplemental Figure 4. Graphical Representation of the *SMR5* and *SMR7* T-DNA Insertion.

Supplemental Figure 5. *SMR5* and *SMR7* Expression Levels in Response to High-Light Treatment.

Supplemental Figure 6. Relative Root Growth of $SMR5^{KO}$, $SMR7^{KO}$, and $SMR5^{KO}$ $SMR7^{KO}$ Plants upon HU Treatment.

Supplemental Table 1. Annotated *Arabidopsis SIM/SMR* Genes.

Supplemental Table 2. DNA Ploidy Level Distribution in Transgenic Plants Overexpressing *SMR4*, *SMR5*, or *SMR7*.

Supplemental Table 3. List of Primers Used for Cloning, Genotyping, and RT-PCR.

Supplemental Data Set 1. Meta-Analysis of Genes Induced in Multiple DNA Damage Experiments.

ACKNOWLEDGMENTS

We thank Annick Bleys for help in preparing the article, Maheshi Dassanayake for pointing out the misannotation of the *SMR5* transcript, and Lorin Spruyt and Frank Van Breusegem for use of the high-light infrastructure. This work was supported by Ghent University (Multi-disciplinary Research Partnership "Bioinformatics: from nucleotides to networks"), by the Interuniversity Attraction Poles Programme (IUAP P7/29 "MARS"), initiated by the Belgian Science Policy Office, and by a grant from the Research Foundation-Flanders (G.0C72.14N). T.C. is a Post-doctoral Fellow of the Research Foundation-Flanders. D.Y. is indebted to the China Scholarship Council (CSC File 2009685045) for a predoctoral scholarship. M.U. was supported by MEXT KAKENHI Grant 22119009 and JST, Core Research for Evolutional Science and Technology.

AUTHOR CONTRIBUTIONS

D.Y., C.L.A.K., T.C., S.V., A.B., M.U., and L.D.V. conceived and designed the research. D.Y., C.L.A.K., T.C., S.V., N.T., Y.O., T.E., K.O.Y., H.V.d.D., and A.B. performed the experiments. D.Y., C.L.A.K., T.C., S.A., N.T., J.L., A.B., M.U., and L.D.V. analyzed the data and wrote the article. All authors read, revised, and approved the article.

Received September 25, 2013; revised November 14, 2013; accepted December 20, 2013; published January 7, 2014.

REFERENCES

Abraham, R.T. (2001). Cell cycle checkpoint signaling through the ATM and ATR kinases. Genes Dev. **15:** 2177–2196.

Adachi, S., et al. (2011). Programmed induction of endoreduplication by DNA double-strand breaks in *Arabidopsis*. Proc. Natl. Acad. Sci. USA **108:** 10004–10009.

Amor, Y., Babiychuk, E., Inzé, D., and Levine, A. (1998). The involvement of poly(ADP-ribose) polymerase in the oxidative stress responses in plants. FEBS Lett. **440:** 1–7.

Bartek, J., and Lukas, J. (2001). Pathways governing G1/S transition and their response to DNA damage. FEBS Lett. **490:** 117–122.

Beeckman, T., and Engler, G. (1994). An easy technique for the clearing of histochemically stained plant tissue. Plant Mol. Biol. Rep. **12:** 37–42.

Beers, R.F., Jr., and Sizer, I.W. (1952). A spectrophotometric method for measuring the breakdown of hydrogen peroxide by catalase. J. Biol. Chem. **195:** 133–140.

Boudolf, V., et al. (2009). CDKB1;1 forms a functional complex with CYCA2;3 to suppress endocycle onset. Plant Physiol. **150:** 1482–1493.

Boudolf, V., Vlieghe, K., Beemster, G.T.S., Magyar, Z., Torres Acosta, J.A., Maes, S., Van Der Schueren, E., Inzé, D., and De Veylder, L. (2004). The plant-specific cyclin-dependent kinase CDKB1;1 and transcription factor E2Fa-DPa control the balance of mitotically dividing and endoreduplicating cells in *Arabidopsis*. Plant Cell **16:** 2683–2692.

Cadet, J., Douki, T., Ravanat, J.-L., and Wagner, J.R. (2012). Measurement of oxidatively generated base damage to nucleic acids in cells: Facts and artifacts. Bioanal. Rev. **4:** 55–74.

Chaturvedi, P., et al. (1999). Mammalian Chk2 is a downstream effector of the ATM-dependent DNA damage checkpoint pathway. Oncogene **18:** 4047–4054.

Che, F.-S., Nakajima, Y., Tanaka, N., Iwano, M., Yoshida, T., Takayama, S., Kadota, I., and Isogai, A. (2000). Flagellin from an incompatible strain of *Pseudomonas avenae* induces a resistance response in cultured rice cells. J. Biol. Chem. **275:** 32347–32356.

Chen, G.X., and Asada, K. (1990). Hydroxyurea and p-aminophenol are the suicide inhibitors of ascorbate peroxidase. J. Biol. Chem. **265:** 2775–2781.

Chen, Y., and Sanchez, Y. (2004). Chk1 in the DNA damage response: Conserved roles from yeasts to mammals. DNA Repair (Amst.) **3:** 1025–1032.

Churchman, M.L., et al. (2006). SIAMESE, a plant-specific cell cycle regulator, controls endoreplication onset in *Arabidopsis thaliana*. Plant Cell **18:** 3145–3157.

Clough, S.J., and Bent, A.F. (1998). Floral dip: A simplified method for *Agrobacterium*-mediated transformation of *Arabidopsis thaliana*. Plant J. **16:** 735–743.

Cools, T., Iantcheva, A., Maes, S., Van den Daele, H., and De Veylder, L. (2010). A replication stress-induced synchronization method for *Arabidopsis thaliana* root meristems. Plant J. **64:** 705–714.

Cools, T., Iantcheva, A., Weimer, A.K., Boens, S., Takahashi, N., Maes, S., Van den Daele, H., Van Isterdael, G., Schnittger, A., and De Veylder, L. (2011). The *Arabidopsis thaliana* checkpoint kinase WEE1 protects against premature vascular differentiation during replication stress. Plant Cell **23:** 1435–1448.

Culligan, K., Tissier, A., and Britt, A. (2004). ATR regulates a G2-phase cell-cycle checkpoint in *Arabidopsis thaliana*. Plant Cell **16:** 1091–1104.

Culligan, K.M., Robertson, C.E., Foreman, J., Doerner, P., and Britt, A.B. (2006). ATR and ATM play both distinct and additive roles in response to ionizing radiation. Plant J. **48:** 947–961.

De Clercq, A., and Inzé, D. (2006). Cyclin-dependent kinase inhibitors in yeast, animals, and plants: a functional comparison. Crit. Rev. Biochem. Mol. Biol. **41:** 293–313.

De Schutter, K., Joubès, J., Cools, T., Verkest, A., Corellou, F., Babiychuk, E., Van Der Schueren, E., Beeckman, T., Kushnir, S., Inzé, D., and De Veylder, L. (2007). *Arabidopsis* WEE1 kinase controls cell cycle arrest in response to activation of the DNA integrity checkpoint. Plant Cell **19:** 211–225.

De Veylder, L., Beeckman, T., Beemster, G.T.S., Krols, L., Terras, F., Landrieu, I., van der Schueren, E., Maes, S., Naudts, M., and Inzé, D. (2001). Functional analysis of cyclin-dependent kinase inhibitors of *Arabidopsis*. Plant Cell **13:** 1653–1668.

DePaoli, H.C., Brito, M.S., Quiapim, A.C., Teixeira, S.P., Goldman, G.H., Dornelas, M.C., and Goldman, M.H.S. (2011). Stigma/style cell cycle inhibitor 1 (SCI1), a tissue-specific cell cycle regulator that controls upper pistil development. New Phytol. **190:** 882–895.

DePaoli, H.C., Goldman, G.H., and Goldman, M.-H.S. (2012). SCI1, the first member of the tissue-specific inhibitors of CDK (TIC) class,

is probably connected to the auxin signaling pathway. Plant Signal. Behav. **7:** 53–58.

Dewitte, W., and Murray, J.A.H. (2003). The plant cell cycle. Annu. Rev. Plant Biol. **54:** 235–264.

Davletova, S., Rizhsky, L., Liang, H., Shengqiang, Z., Oliver, D.J., Coutu, J., Shulaev, V., Schlauch, K., and Mittler, R. (2005). Cytosolic ascorbate peroxidase 1 is a central component of the reactive oxygen gene network of *Arabidopsis*. Plant Cell **17:** 268–281.

Dissmeyer, N., Weimer, A.K., Pusch, S., De Schutter, K., Alvim Kamei, C.L., Nowack, M.K., Novak, B., Duan, G.-L., Zhu, Y.-G., De Veylder, L., and Schnittger, A. (2009). Control of cell proliferation, organ growth, and DNA damage response operate independently of dephosphorylation of the *Arabidopsis* Cdk1 homolog CDKA;1. Plant Cell **21:** 3641–3654.

Dizdaroglu, M., Jaruga, P., Birincioglu, M., and Rodriguez, H. (2002). Free radical-induced damage to DNA: Mechanisms and measurement. Free Radic. Biol. Med. **32:** 1102–1115.

Dubacq, C., Chevalier, A., Courbeyrette, R., Petat, C., Gidrol, X., and Mann, C. (2006). Role of the iron mobilization and oxidative stress regulons in the genomic response of yeast to hydroxyurea. Mol. Genet. Genomics **275:** 114–124.

Dunand, C., Crèvecoeur, M., and Penel, C. (2007). Distribution of superoxide and hydrogen peroxide in *Arabidopsis* root and their influence on root development: Possible interaction with peroxidases. New Phytol. **174:** 332–341.

Francis, D. (2011). A commentary on the G2/M transition of the plant cell cycle. Ann. Bot. (Lond.) **107:** 1065–1070.

French, A.P., Wilson, M.H., Kenobi, K., Dietrich, D., Voß, U., Ubeda-Tomás, S., Pridmore, T.P., and Wells, D.M. (2012). Identifying biological landmarks using a novel cell measuring image analysis tool: Cell-o-Tape. Plant Methods **8:** 7.

Galbraith, D.W., Harkins, K.R., and Knapp, S. (1991). Systemic endopolyploidy in *Arabidopsis thaliana*. Plant Physiol. **96:** 985–989.

Garcia, V., Bruchet, H., Camescasse, D., Granier, F., Bouchez, D., and Tissier, A. (2003). *AtATM* is essential for meiosis and the somatic response to DNA damage in plants. Plant Cell **15:** 119–132.

Gendrel, A.-V., Lippman, Z., Martienssen, R., and Colot, V. (2005). Profiling histone modification patterns in plants using genomic tiling microarrays. Nat. Methods **2:** 213–218.

Guo, Z., Kozlov, S., Lavin, M.F., Person, M.D., and Paull, T.T. (2010). ATM activation by oxidative stress. Science **330:** 517–521.

Hruz, T., Laule, O., Szabo, G., Wessendorp, F., Bleuler, S., Oertle, L., Widmayer, P., Gruissem, W., and Zimmermann, P. (2008). Genevestigator v3: A reference expression database for the meta-analysis of transcriptomes. Adv. Bioinforma. **2008:** 420747.

Irizarry, R.A., Hobbs, B., Collin, F., Beazer-Barclay, Y.D., Antonellis, K.J., Scherf, U., and Speed, T.P. (2003). Exploration, normalization, and summaries of high density oligonucleotide array probe level data. Biostatistics **4:** 249–264.

Juul, T., Malolepszy, A., Dybkaer, K., Kidmose, R., Rasmussen, J.T., Andersen, G.R., Johnsen, H.E., Jørgensen, J.-E., and Andersen, S.U. (2010). The *in vivo* toxicity of hydroxyurea depends on its direct target catalase. J. Biol. Chem. **285:** 21411–21415.

Karimi, M., Bleys, A., Vanderhaeghen, R., and Hilson, P. (2007). Building blocks for plant gene assembly. Plant Physiol. **145:** 1183–1191.

Karimi, M., Inzé, D., and Depicker, A. (2002). GATEWAY™ vectors for *Agrobacterium*-mediated plant transformation. Trends Plant Sci. **7:** 193–195.

Kinoshita, E., Kinoshita-Kikuta, E., Takiyama, K., and Koike, T. (2006). Phosphate-binding tag, a new tool to visualize phosphorylated proteins. Mol. Cell. Proteomics **5:** 749–757.

Kurz, E.U., and Lees-Miller, S.P. (2004). DNA damage-induced activation of ATM and ATM-dependent signaling pathways. DNA Repair (Amst.) **3:** 889–900.

Lee, M.G., and Nurse, P. (1987). Complementation used to clone a human homologue of the fission yeast cell cycle control gene *cdc2*. Nature **327:** 31–35.

Minami, E., Kuchitsu, K., He, D.-Y., Kouchi, H., Midoh, N., Ohtsuki, Y., and Shibuya, N. (1996). Two novel genes rapidly and transiently activated in suspension-cultured rice cells by treatment with *N*-acetylchitoheptaose, a biotic elicitor for phytoalexin production. Plant Cell Physiol. **37:** 563–567.

Mittler, R. (2002). Oxidative stress, antioxidants and stress tolerance. Trends Plant Sci. **7:** 405–410.

Mittler, R., Vanderauwera, S., Gollery, M., and Van Breusegem, F. (2004). Reactive oxygen gene network of plants. Trends Plant Sci. **9:** 490–498.

Mittler, R., Vanderauwera, S., Suzuki, N., Miller, G., Tognetti, V.B., Vandepoele, K., Gollery, M., Shulaev, V., and Van Breusegem, F. (2011). ROS signaling: The new wave? Trends Plant Sci. **16:** 300–309.

Murashige, T., and Skoog, F. (1962). A revised medium for rapid growth and bio assays with tobacco tissue cultures. Physiol. Plant. **15:** 473–497.

Murata, N., Allakhverdiev, S.I., and Nishiyama, Y. (2012). The mechanism of photoinhibition in vivo: Re-evaluation of the roles of catalase, α-tocopherol, non-photochemical quenching, and electron transport. Biochim. Biophys. Acta **1817:** 1127–1133.

Norbury, C., and Nurse, P. (1992). Animal cell cycles and their control. Annu. Rev. Biochem. **61:** 441–470.

Nowack, M.K., Harashima, H., Dissmeyer, N., Zhao, X., Bouyer, D., Weimer, A.K., De Winter, F., Yang, F., and Schnittger, A. (2012). Genetic framework of cyclin-dependent kinase function in *Arabidopsis*. Dev. Cell **22:** 1030–1040.

Nowack, M.K., Ungru, A., Bjerkan, K.N., Grini, P.E., and Schnittger, A. (2010). Reproductive cross-talk: Seed development in flowering plants. Biochem. Soc. Trans. **38:** 604–612.

Nyholm, S., Mann, G.J., Johansson, A.G., Bergeron, R.J., Gräslund, A., and Thelander, L. (1993). Role of ribonucleotide reductase in inhibition of mammalian cell growth by potent iron chelators. J. Biol. Chem. **268:** 26200–26205.

Peres, A., et al. (2007). Novel plant-specific cyclin-dependent kinase inhibitors induced by biotic and abiotic stresses. J. Biol. Chem. **282:** 25588–25596.

Preuss, S.B., and Britt, A.B. (2003). A DNA-damage-induced cell cycle checkpoint in Arabidopsis. Genetics **164:** 323–334.

Reichheld, J.-P., Vernoux, T., Lardon, F., Van Montagu, M., and Inzé, D. (1999). Specific checkpoints regulate plant cell cycle progression in response to oxidative stress. Plant J. **17:** 647–656.

Ricaud, L., Proux, C., Renou, J.-P., Pichon, O., Fochesato, S., Ortet, P., and Montané, M.-H. (2007). ATM-mediated transcriptional and developmental responses to γ-rays in *Arabidopsis*. PLoS ONE **2:** e430.

Riou-Khamlichi, C., Menges, M., Healy, J.M.S., and Murray, J.A.H. (2000). Sugar control of the plant cell cycle: Differential regulation of *Arabidopsis* D-type cyclin gene expression. Mol. Cell. Biol. **20:** 4513–4521.

Roeder, A.H.K., Chickarmane, V., Cunha, A., Obara, B., Manjunath, B.S., and Meyerowitz, E.M. (2010). Variability in the control of cell division underlies sepal epidermal patterning in *Arabidopsis thaliana*. PLoS Biol. **8:** e1000367.

Roldán-Arjona, T., and Ariza, R.R. (2009). Repair and tolerance of oxidative DNA damage in plants. Mutat. Res. **681:** 169–179.

Rozan, L.M., and El-Deiry, W.S. (2007). p53 downstream target genes and tumor suppression: A classical view in evolution. Cell Death Differ. **14:** 3–9.

Sherr, C.J., and Roberts, J.M. (1995). Inhibitors of mammalian G1 cyclin-dependent kinases. Genes Dev. **9:** 1149–1163.

Shieh, S.-Y., Ahn, J., Tamai, K., Taya, Y., and Prives, C. (2000). The human homologs of checkpoint kinases Chk1 and Cds1 (Chk2) phosphorylate p53 at multiple DNA damage-inducible sites. Genes Dev. **14:** 289–300.

Tsukagoshi, H. (2012). Defective root growth triggered by oxidative stress is controlled through the expression of cell cycle-related genes. Plant Sci. **197:** 30–39.

Tsukagoshi, H., Busch, W., and Benfey, P.N. (2010). Transcriptional regulation of ROS controls transition from proliferation to differentiation in the root. Cell **143:** 606–616.

Tusher, V.G., Tibshirani, R., and Chu, G. (2001). Significance analysis of microarrays applied to the ionizing radiation response. Proc. Natl. Acad. Sci. USA **98:** 5116–5121.

Vandenabeele, S., Vanderauwera, S., Vuylsteke, M., Rombauts, S., Langebartels, C., Seidlitz, H.K., Zabeau, M., Van Montagu, M., Inzé, D., and Van Breusegem, F. (2004). Catalase deficiency drastically affects gene expression induced by high light in *Arabidopsis thaliana*. Plant J. **39:** 45–58.

Vanderauwera, S., Suzuki, N., Miller, G., van de Cotte, B., Morsa, S., Ravanat, J.-L., Hegie, A., Triantaphylidès, C., Shulaev, V., Van Montagu, M.C.E., Van Breusegem, F., and Mittler, R. (2011). Extranuclear protection of chromosomal DNA from oxidative stress. Proc. Natl. Acad. Sci. USA **108:** 1711–1716.

Van Leene, J., et al. (2010). Targeted interactomics reveals a complex core cell cycle machinery in *Arabidopsis thaliana*. Mol. Syst. Biol. **6:** 397.

Vernoux, T., Wilson, R.C., Seeley, K.A., Reichheld, J.-P., Muroy, S., Brown, S., Maughan, S.C., Cobbett, C.S., Van Montagu, M., Inzé, D., May, M.J., and Sung, Z.R. (2000). The *ROOT MERISTEMLESS1/CADMIUM SENSITIVE2* gene defines a glutathione-dependent pathway involved in initiation and maintenance of cell division during postembryonic root development. Plant Cell **12:** 97–110.

Wang, H., Qi, Q., Schorr, P., Cutler, A.J., Crosby, W.L., and Fowke, L.C. (1998). ICK1, a cyclin-dependent protein kinase inhibitor from *Arabidopsis thaliana* interacts with both Cdc2a and CycD3, and its expression is induced by abscisic acid. Plant J. **15:** 501–510.

Wang, H., Zhou, Y., Gilmer, S., Whitwill, S., and Fowke, L.C. (2000). Expression of the plant cyclin-dependent kinase inhibitor ICK1 affects cell division, plant growth and morphology. Plant J. **24:** 613–623.

Yoshiyama, K., Conklin, P.A., Huefner, N.D., and Britt, A.B. (2009). Suppressor of gamma response 1 (*SOG1*) encodes a putative transcription factor governing multiple responses to DNA damage. Proc. Natl. Acad. Sci. USA **106:** 12843–12848.

Yoshiyama, K.O., Kobayashi, J., Ogita, N., Ueda, M., Kimura, S., Maki, H., and Umeda, M. (2013). ATM-mediated phosphorylation of SOG1 is essential for the DNA damage response in *Arabidopsis*. EMBO Rep. **14:** 817–822.

Zhou, B.-B., and Elledge, S.J. (2000). The DNA damage response: Putting checkpoints in perspective. Nature **408:** 433–439.